





## Article

# Monitoring In Vitro and In Vivo Aroma Release of Espresso Coffees with Proton-Transfer-Reaction Time-of-Flight Mass Spectrometry

Andrea Romano <sup>1</sup>, Luca Cappellin <sup>1</sup>, Sara Bogialli <sup>1</sup> , Paolo Pastore <sup>1</sup> , Luciano Navarini <sup>2</sup>   
and Franco Biasioli <sup>3,\*</sup> 

<sup>1</sup> Department of Chemical Sciences, University of Padova, Via Marzolo, 1, 35131 Padova, Italy

<sup>2</sup> Illycaffè S.p.A., Via Flavia 110, 34147 Trieste, Italy

<sup>3</sup> Research and Innovation Centre, Edmund Mach Foundation, Via Edmund Mach, 1, 38010 San Michele all'Adige, Italy

\* Correspondence: franco.biasioli@fmach.it

**Abstract:** This work presents in vitro and in vivo aroma release analysis of three espresso coffees carried out by PTR-ToF-MS headspace and nosespace analysis, respectively. The products were *C. arabica* coffees prepared using an espresso coffee machine: a low-caffeine *C. arabica* var. *laurina* light roast, a low-caffeine *C. arabica* var. *laurina* dark roast, and a single-origin coffee from Ethiopia which were roasted to a medium roast degree. Headspace analysis allowed for discrimination between coffees with a prediction accuracy of 92% or higher. Relevant discriminating compounds were related to the roasting degree and varietal compounds. Coffee nosespace consisted of 35 mass peaks overall. Despite this relatively low number of detected peaks, coffee discrimination was still possible with  $\geq 93\%$  accuracy. The compounds most relevant to the discrimination were those related to the roasting degree. Major differences—both qualitative and quantitative—were found between headspace and nosespace profiles.

**Keywords:** aroma release; headspace; nosespace; espresso coffee; PTR-ToF-MS



**Citation:** Romano, A.; Cappellin, L.; Bogialli, S.; Pastore, P.; Navarini, L.; Biasioli, F. Monitoring in Vitro and in Vivo Aroma Release of Espresso Coffees with Proton-Transfer-Reaction Time-of-Flight Mass Spectrometry. *Appl. Sci.* **2022**, *12*, 10272. <https://doi.org/10.3390/app122010272>

Academic Editors: Claire Turner, Célia Lourenço and Ramón González-Méndez

Received: 27 September 2022

Accepted: 10 October 2022

Published: 12 October 2022

**Publisher's Note:** MDPI stays neutral with regard to jurisdictional claims in published maps and institutional affiliations.



**Copyright:** © 2022 by the authors. Licensee MDPI, Basel, Switzerland. This article is an open access article distributed under the terms and conditions of the Creative Commons Attribution (CC BY) license (<https://creativecommons.org/licenses/by/4.0/>).

## 1. Introduction

The characterization of coffees with special flavor characteristics is a growing interest to most coffee companies. When a package of coffee is opened, the first appreciation is its aroma [1,2] which drives choices and preferences before and after buying a product. This first-created aroma sensation is called orthonasal perception [1] or above-the-food aroma [3], and it involves the direct transport to the nose of food volatile organic compounds (VOCs).

In most cases, the first aroma perception plays a major role in consumer preferences. However, the flavor characteristics of a particular coffee keep their significance during consumption as well. The so-called “retronasal perception” is initiated by the VOCs in the exhaled breath, which reach the olfactory system after swallowing [1,2]. In both cases of aroma perception, the VOCs reach the olfactory bulb in the nose. However, the interpretation of odor perception highly depends on the route followed by the volatiles, physical properties of the aroma compounds, food composition, texture and interactions with the matrix components, and factors related to the physiology of the consumers [1,4,5].

The monitoring of retronasal (or in vivo) aroma release, also known as “nosespace analysis”, can be carried out using APCI-MS, PTR-MS, or SIFT-MS [6]. Proton-transfer-reaction mass spectrometry (PTR-MS) was first used to monitor coffee aroma release with in-mouth and nosespace measurements [3,7] with a focus on inter- and intra-individual differences among consumers and release mechanisms. PTR-MS was later applied to the investigation of the effect of coffee foam on VOC release in espresso coffees [8], the study

of inter-individual differences in coffee aroma release [9], and the correlation between time-resolved aroma release and retronasal perception [10].

Untargeted analysis by means of PTR-ToF-MS has been carried out successfully with the aim of differentiating coffees based on their headspace composition. For example, it was possible to discriminate between Arabica and Robusta [11] or among different Robusta blends based on their geographical origin [12,13].

The aim of this study was to verify whether it was possible to discriminate espresso coffees based on their nosespace profiles. The same products were also analyzed by means of headspace analysis. This allowed performing a thorough comparison between in vivo and in vitro aroma release. Two Arabica espresso coffees, naturally low in caffeine, and a single-origin Ethiopian coffee were analyzed. PTR-ToF-MS was capable of characterizing both in vivo and in vitro release, highlighting key differences between the three espresso coffees. However, the key differentiating aroma compounds and the composition of the respective release profiles significantly differ between in vitro and in vivo.

## 2. Materials and Methods

### 2.1. Coffee Samples

Green *C. arabica* var. *laurina* beans (geographical origin: El Salvador) were roasted in a pilot plant (8.0 kg batch) at two different intensities, as determined by color measurement (Colorette 3 B, Probat): coffee A (color  $108 \pm 3$  A.U. corresponding to light roast, LR) and coffee B (color  $82 \pm 3$  A.U. corresponding to dark roast, DR). Coffees A and B, after proper grinding, were packed in capsules by industrial process (Iperespresso, illycaffè s.p.a., Trieste, Italy). Commercially available Monoarabica™ single-origin Iperespresso capsules coffee from Ethiopia (medium roast degree, MR) was used and hereafter named Coffee E. The two samples of “laurina” coffee (i.e., coffee A and coffee B) cover a wide range of degrees of roasting (from very light to very dark) and were used precisely for this. Coffee E (Ethiopian origin and intermediate degree of roasting) was chosen because it was particularly interesting from an aromatic point of view. As seen in previous works [12–14], Ethiopian coffee is characterized by a higher content of monoterpenes, and this makes it particularly aromatic. Espresso coffee samples were prepared by using an Iperespresso coffee machine (Iperespresso X7.1, illycaffè s.p.a.) by following a two-phase extraction process (pre-infusion and percolation); water temperature, pressure, and extraction time were precisely calibrated before brewing. To standardize the coffee beverages, mineral water was used (San Benedetto S.p.A., Italy, composition:  $\text{Ca}^{2+}$  50.3 mg/L,  $\text{Mg}^{2+}$  30.8 mg/L,  $\text{Na}^+$  6.0 mg/L,  $\text{K}^+$  0.9 mg/L). Total extraction time was adjusted to obtain a 30 mL standard espresso cup volume.

### 2.2. PTR-ToF-MS Measurements

A commercial PTR-ToF-MS 8000 instrument (Ionicon Analytik GmbH, Innsbruck, Austria) was used throughout the study. Ionisation was performed at an E/N ratio of 140 Td (drift temperature = 110 °C, drift voltage = 550 V, and drift pressure = 2.33 mbar). Data acquisition was set to 1 cycle  $\text{s}^{-1}$ . For headspace measurements, inlet flow was set to 40 sccm, whereas for nosespace, a flow of 440 sccm was employed, which allowed for a shorter instrumental response time.

### 2.3. Nosespace (NS) Analysis

Nosespace analysis was carried out following a protocol used during previous studies involving coffee nosespace [9,10]. NS analysis was carried out with the help of 3 panelists (2 males and 1 female, age 29–39) in 5 separate sessions and tasting 3 espresso coffees per session (in total 45 NS sessions). Based on previous experience [9], these subjects had proven to generate reproducible NS release profiles; therefore, they were asked to join the present study. All panelists joined every session, and three freshly prepared espresso coffees were served to each panelist in randomized order. Before each nosespace session, coffees were prepared freshly and one by one for each panelist. After preparation, 10-mL coffee

aliquots were taken without the crema and served to the panelists at 55 °C in a polystyrene cup with a lid and a straw. NS sessions were performed according to a pre-defined protocol as follows: 30 s of free breathing (mouth closed), putting the sample in the mouth and swallowing (total 10 s), 2 min of free breathing, mouth rinsing with water (20 s). Breath exhaled through the nose was sampled by applying an ergonomic glass nosepiece directly connected to the PTR-ToF-MS inlet, which was heated at 110 °C. Each NS session lasted around 220 s; for the data analysis the first 150 s were used.

#### 2.4. Headspace (HS) Analysis

Coffee headspace analysis was carried out using a previously developed protocol [10]. On each day of measurement ( $n = 4$ ), 3 extraction replicates were prepared for each coffee sample. In total, 34 HS measurements were performed (namely, 12 coffee A, 11 coffee B, and 11 coffee E; one coffee B and one coffee E had to be discarded due to some technical problems related to data acquisition). The coffee, once prepared, was briefly stirred, and then a 2 mL aliquot (without crema) was immediately transferred into a 22 mL glass vial (Supelco, Bellefonte, PA, USA). After 30 min of equilibration at 40 °C, the vial headspace was measured. Each measurement was obtained by averaging 30 s of acquisition. A multipurpose autosampler (Gerstel GmbH, Mulheim am Ruhr, Germany) was employed for automated coffee HS analysis. The robotic arm of the autosampler was equipped with a headspace syringe, along with a Multiple Headspace Extraction (MHE) tool. The latter was connected to the inlet of the PTR-MS. During headspace sampling, the vial septum is pierced by both the HS syringe and the MHE needle at the same time, and the air sampled by the PTR-MS is replaced by clean air, which is supplied via the headspace syringe.

#### 2.5. Data Analysis

##### 2.5.1. PTR-ToF-MS Spectra Processing

Dead time correction, internal calibration of PTR-ToF-MS data, and subsequent peak extraction steps were performed according to the procedures described elsewhere [15–17] to reach a mass accuracy ( $\leq 0.001 m/z$ ) which is sufficient for sum formula determination, and a dynamic range extending above 1 ppmV. Mass spectra baseline removal was carried out after averaging the whole measurement, and a modified Gaussian was used to fit the data for the purpose of peak detection and peak area extraction. VOC concentration was calculated directly in ppbV (parts per billion in volume) starting from the number of detected ions, using the model developed by Lindinger and co-workers [18]. A constant reaction rate coefficient ( $k_R = 2.0 \times 10^{-9} \text{ cm}^3/\text{s}$ ) was assumed for all ionisation reactions. Mass spectra recording was set in the mass-to-charge ratio range of 15–300  $m/z$ . During sample measurement, no significant decrease in the primary ion amount, as estimated by monitoring ion  $m/z$  21.022, was observed, which indicates that no primary ion depletion took place at any given moment.

##### 2.5.2. NS Data Treatment

After PTR-ToF-MS spectra processing, the unfiltered dataset consisted of 468 mass peaks recorded over 45 NS sessions. The dataset was filtered (or pre-processed) according to the procedure fully described in [10], the key steps of which are the selection of peak-like features to highlight those mass peaks related to release profiles and the elimination of NaN-containing columns to rule out low-quality data. Overall, the final nospace dataset contained 35 mass peaks, each associated with up to six parameters. The parameters were the release maximum (maximum), the area under the curve (area), the median intensity (median), the final intensity (final), the time required to reach maximum intensity (tmax), and the slope of the descending part of the curve (slope). This provided a data matrix consisting of 207 parameters. After this step, ANOVA and post-hoc analysis were carried out by setting a  $p$ -value threshold of 0.01 (after false discovery rate correction). Partial Least Square Discriminant Analysis (PLS-DA) was carried out with the aim of assessing PTR-ToF-MS discrimination capabilities based on NS data and pinpointing key

discriminating variables through the employment of Variable Importance in Projection (VIP) values [19]. The PLS-DA prediction model was built by applying leave-group-out (LGO) cross-validation, where each group consisted of an NS session that was performed on different days.

### 2.5.3. HS Data Treatment

The HS dataset consisted of 593 mass peaks overall. Only peaks whose headspace concentrations exceeded 1 ppbV were selected for further analysis. Signals related to the primary ion (hydronium ion and water clusters) and those due to ion impurities ( $\text{NO}^+$ ,  $\text{O}_2^+$ , etc.) were excluded. This resulted in a data set of 277 mass peaks. ANOVA and post-hoc tests were performed by applying a threshold of 0.01 to  $p$ -values and after false discovery rate correction. The data set was also used for the discrimination of espresso coffees based on HS data through a PLS-DA, which further allowed annotation of the most important variables in discrimination ( $\text{VIP} > 1.5$ ). Similarly to the PLS-DA performed on NS data, the LGO cross-validation approach was applied by using the HS results obtained from measurements carried out on different days.

### 2.5.4. Software

PTR-ToF-MS data processing and statistical analyses (one-way ANOVA and PLS-DA) were performed by using software packages and scripts developed in-house in MATLAB (MathWorks, Natick, MA, USA) and R Programming Language [20].

## 3. Results and Discussion

### 3.1. In Vitro Aroma Release

Following one-way ANOVA, 222 mass peaks showed significant differences between the three espresso coffee samples. Higher roasting degrees are known to increase VOC contents in coffee beans [21] as well as in capsule coffee brews [14], and the results obtained here are in agreement with these findings. Coffee A showed the lowest volatile intensities for all the significantly different mass peaks. The highest concentrations were instead found in coffee B alone (171 peaks), coffee B and coffee E together (44 peaks), or coffee E alone (7 peaks). Table S1 (Supplementary Material) summarises the results of one-way ANOVA and post-hoc analysis.

PLS-DA resulted in excellent discrimination of coffee samples. The confusion matrix and the score plot of PLS-DA are displayed in Table 1 and Figure 1, respectively. Coffee B and E were correctly predicted 100% of the time, whereas coffee A was misidentified once as coffee E. In addition to the good discrimination provided by PLS-DA, it was possible to annotate mass peaks with VIP values higher than 1.5, which were the most significant mass peaks for discrimination of the coffee samples. Table 2 gives a list of these 15 mass peaks with a sum formula, tentative identifications, and average concentrations for each coffee sample. In addition to Table 2, these mass peaks can be visualized in Figure 1.

**Table 1.** Confusion matrices generated by PLS-DA (leave-group-out cross-validation). Models based on headspace and nosespace data are presented (left and right, respectively).

	Headspace			Nosespace			
	Predicted			Predicted			
	Coffee A	Coffee B	Coffee E	Coffee A	Coffee B	Coffee E	
Original	Coffee A	11	0	1	14	0	1
	Coffee B	0	11	0	0	14	1
	Coffee E	0	0	11	0	0	15

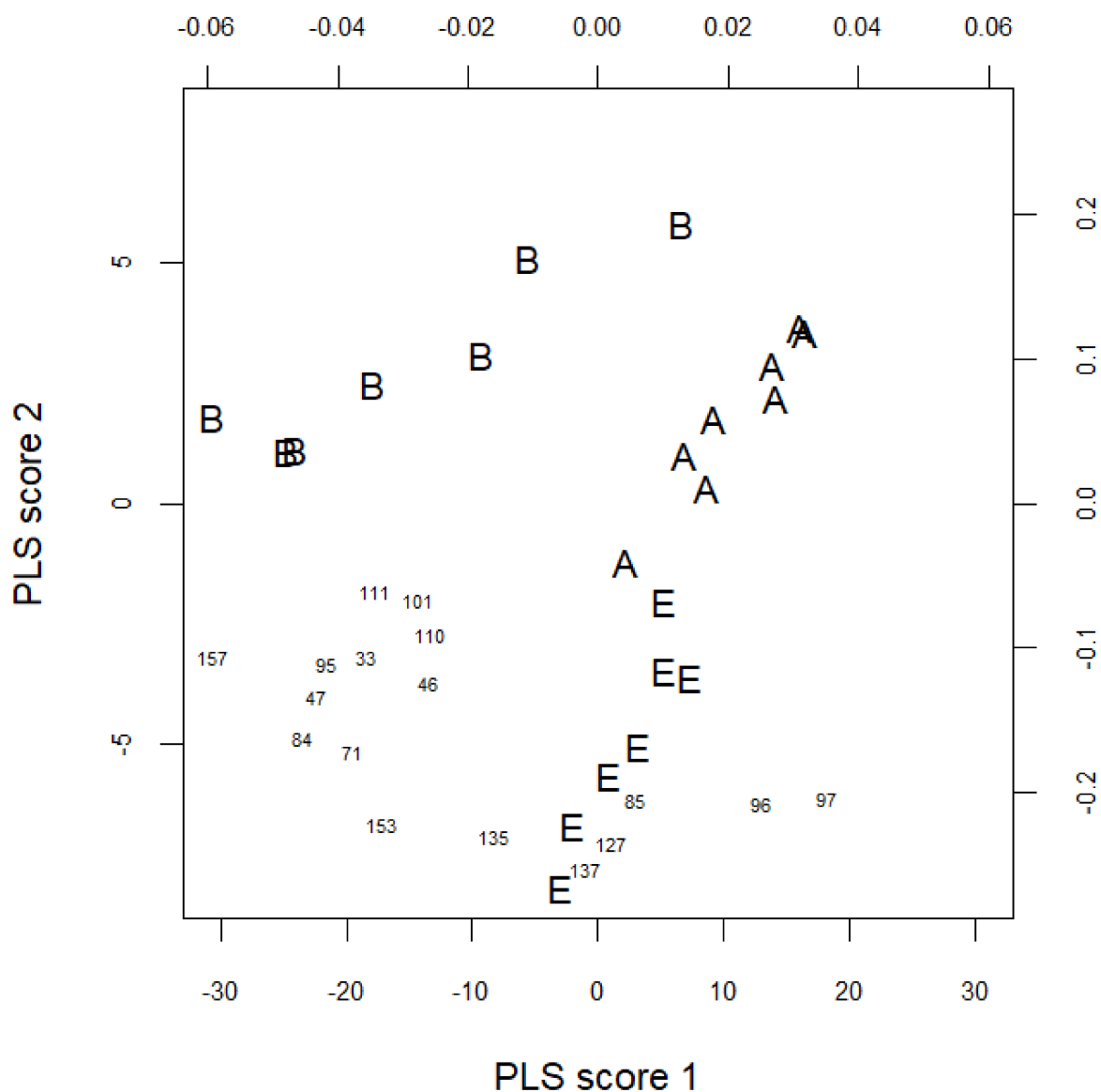


**Figure 1.** Graphical output of the Principal Least Square Discriminant Analysis of the espresso coffee headspace analysis. In the score plot, letters depict samples, and highly influential variables (VIP scores higher than 1.5) are represented by means of the corresponding nominal masses.

The main differences between coffee A and B were observed in the intensity of most mass peaks. The most discriminating mass peaks for coffee E are  $m/z$  135.117, 153.130, 85.104, 97.028, 127.149, and 137.134, characterized by the highest intensities. Among them,  $m/z$  137.134 and 153.130 can be tentatively identified as various monoterpenes and decadienal, which are responsible for fruity and citrus notes, respectively [22,23]. Flowery, fruity, and citrus notes have been highly associated with Ethiopian coffee aroma, and the discrimination of this coffee for the related mass peaks are in accordance with our previous findings [12,13]. Similarly, a recent study performed on coffee powders and capsule coffee brews [14] has shown that terpene profiles are important in the discrimination of mono-origin varietal coffees, with Ethiopian coffee being particularly rich in terpenes.

### 3.2. In Vivo Aroma Release

Following one-way ANOVA, 16 parameters showed significant differences between two or more coffee types. Table S2 (Supplementary Material) summarises the results of one-way ANOVA and post-hoc analysis. A good discrimination of the coffee samples

based on the extracted nospace parameters (Figure 2) was obtained by PLS-DA with 93–100% correct predictions (Table 1); coffee E was always predicted correctly, whereas coffee A and coffee B were misidentified one time each as coffee E. These results indicate a good reproducibility obtained from NS sessions performed on different days, thanks to panelist selection.

**Table 2.** Selected headspace mass peaks significant for discrimination (VIP > 1.5). Means and standard deviations are reported for each sample. *p*-values were obtained on the basis of one-way ANOVA and corrected, taking into account the false discovery rate. Superscript annotations are used to display differences between coffees; therefore, when two values are annotated by different letters, this denotes the pairwise statistically significant difference (Tukey's HSD).

Measured Mass <i>m/z</i> (Th)	Sum Formula	Tentative Identification	Coffee A (ppbV)	Coffee B (ppbV)	Coffee E (ppbV)	<i>p</i> -Value
33.033	CH <sub>5</sub> O <sup>+</sup>	Methanol	6157 ± 1651 <sup>a</sup>	10,263 ± 3610 <sup>b</sup>	11,102 ± 2342 <sup>b</sup>	<10 <sup>−3</sup>
46.038	C <sup>[13]</sup> CH <sub>5</sub> O <sup>+</sup>	<sup>13</sup> C isotope acetaldehyde	262 ± 79 <sup>a</sup>	385 ± 107 <sup>b</sup>	478 ± 110 <sup>b</sup>	<10 <sup>−3</sup>
47.050	C <sub>2</sub> H <sub>7</sub> O <sup>+</sup>	Ethanol	32 ± 8 <sup>a</sup>	51 ± 14 <sup>b</sup>	52 ± 9 <sup>b</sup>	<10 <sup>−3</sup>
71.087	C <sub>5</sub> H <sub>11</sub> <sup>+</sup>	Terpene fragment	15 ± 5 <sup>a</sup>	31 ± 9 <sup>b</sup>	37 ± 9 <sup>b</sup>	<10 <sup>−3</sup>
84.088	C <sub>5</sub> <sup>[13]</sup> CH <sub>11</sub> <sup>+</sup>	<sup>13</sup> C isotope fragment (diverse origin)	1.8 ± 1.1 <sup>a</sup>	4.6 ± 1.2 <sup>b</sup>	5.8 ± 0.8 <sup>b</sup>	<10 <sup>−3</sup>
85.103	C <sub>6</sub> H <sub>13</sub> <sup>+</sup>	Methyl-butene/aldehyde fragment	4.5 ± 2.4 <sup>a</sup>	4.8 ± 3.7 <sup>a</sup>	13.9 ± 6.1 <sup>b</sup>	<10 <sup>−3</sup>
95.007	C <sub>2</sub> H <sub>7</sub> S <sub>2</sub> <sup>+</sup>	Dimethyl-disulfide	132 ± 42 <sup>a</sup>	215 ± 48 <sup>b</sup>	235 ± 43 <sup>b</sup>	<10 <sup>−3</sup>
97.028	C <sub>5</sub> H <sub>5</sub> O <sub>2</sub> <sup>+</sup>	Furfural	2925 ± 998 <sup>a</sup>	2461 ± 850 <sup>a</sup>	5280 ± 1111 <sup>b</sup>	<10 <sup>−3</sup>
101.060	C <sub>5</sub> H <sub>9</sub> O <sub>2</sub> <sup>+</sup>	Pentanedione/methyl-tetrahydrofuranone	988 ± 324 <sup>a</sup>	1504 ± 524 <sup>b</sup>	1619 ± 407 <sup>b</sup>	<10 <sup>−3</sup>
111.044	C <sub>6</sub> H <sub>7</sub> O <sub>2</sub> <sup>+</sup>	Acetyl-furan/methyl-furfural	1641 ± 554 <sup>a</sup>	2556 ± 827 <sup>b</sup>	2579 ± 491 <sup>b</sup>	<10 <sup>−3</sup>
127.150	N.a.	N.a.	0.6 ± 0.3 <sup>a</sup>	0.8 ± 0.4 <sup>a</sup>	2.3 ± 0.8 <sup>b</sup>	<10 <sup>−3</sup>
135.117	C <sub>10</sub> H <sub>15</sub> <sup>+</sup>	Terpene fragment	1.7 ± 0.6 <sup>a</sup>	2.8 ± 0.8 <sup>b</sup>	5.4 ± 1.2 <sup>c</sup>	<10 <sup>−3</sup>
137.134	C <sub>10</sub> H <sub>17</sub> <sup>+</sup>	Various monoterpenes	4.9 ± 1.6 <sup>a</sup>	7.6 ± 2.5 <sup>a</sup>	22.3 ± 6.3 <sup>b</sup>	<10 <sup>−3</sup>
153.131	C <sub>10</sub> H <sub>17</sub> O <sup>+</sup>	Decadienal	3.1 ± 1.0 <sup>a</sup>	7.2 ± 1.6 <sup>b</sup>	11.4 ± 2.1 <sup>c</sup>	<10 <sup>−3</sup>
157.124	C <sub>9</sub> H <sub>17</sub> O <sub>2</sub> <sup>+</sup>	Hydroxy-nonenal	0.7 ± 0.2 <sup>a</sup>	1.8 ± 0.5 <sup>b</sup>	1.9 ± 0.3 <sup>b</sup>	<10 <sup>−3</sup>

N.a.: Not annotated.

The most important variables in the discrimination (VIP > 1.5) were associated with a handful of mass peaks, as shown in Table 3. Mass peaks significant for discrimination were in total 7, and all of them were associated with volatile compounds formed during coffee roasting [23], suggesting a separation mostly based on roasting degree. No common mass peaks for headspace and nospace discrimination of the coffee samples have been found. The volatile compounds associated with discriminative NS mass peaks are known to have odor descriptors of roasted, smoky, and burnt notes [23].

The most noticeable differences among the mass peaks in Table 3 were due to the absence and/or very low presence of them in coffee A. For instance, the mass peak at *m/z* 98.074, tentatively identified as dimethyl-oxazole, was detected in coffee B alone, whereas mass peaks at *m/z* 82.070 (methyl-pyrrole) and 99.082 (hexenal/methylcyclopentanone) were detected in coffee B and E, and non-detectable in coffee A. These mass peaks were detected in the headspace of coffee A; however, in the exhaled breath, the intensities decreased significantly and/or their concentrations were below the detection limit of the instrument. The most frequent release parameter for NS discrimination was recorded as area, which was related to the total amount of a specific mass peak released within the nospace. The second most common parameter was recorded as slope, which relates to the persistence of the corresponding mass peak within the nospace.



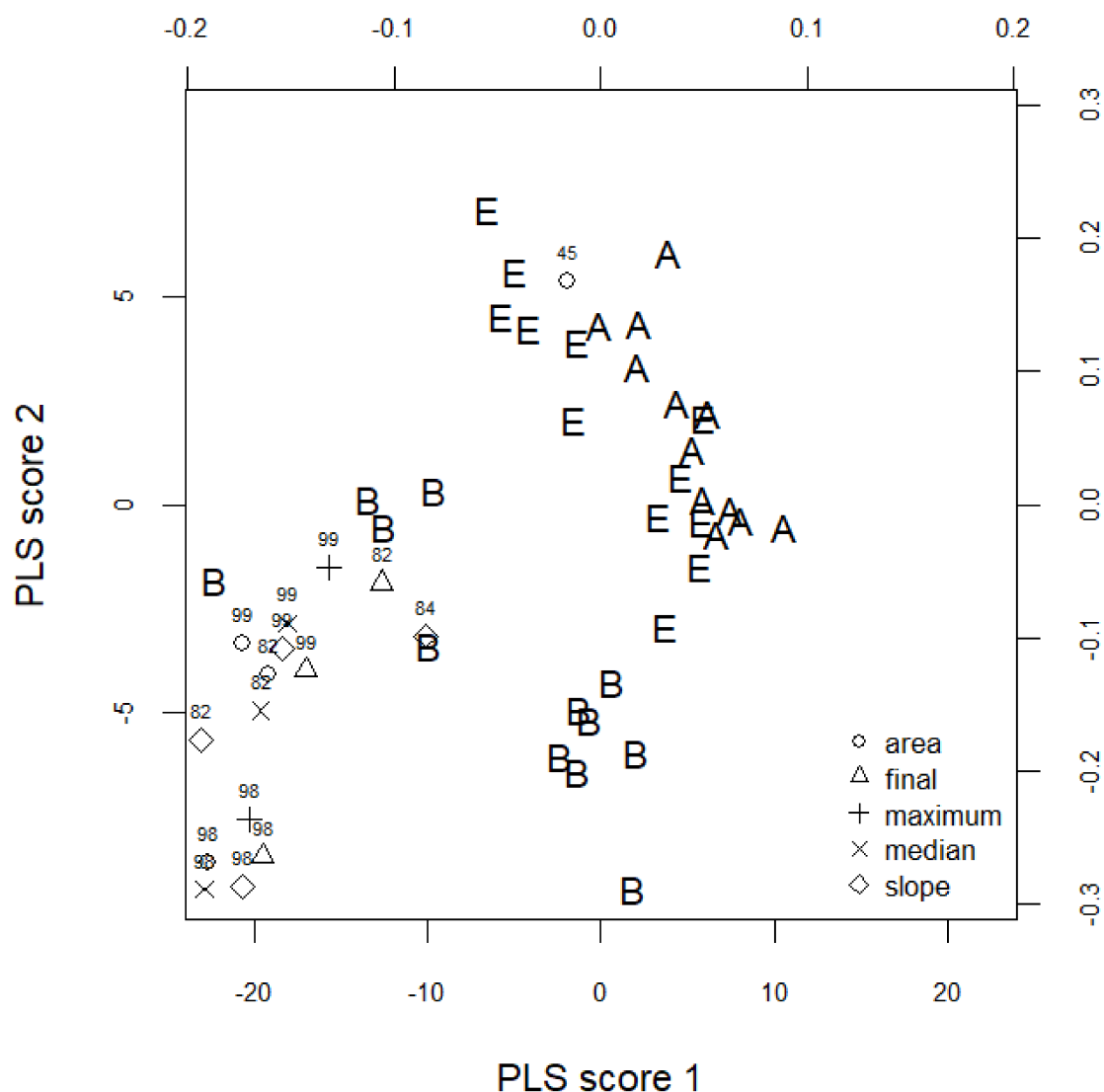


**Figure 2.** Graphical output of the Principal Least Square Discriminant Analysis of the espresso coffee nosespace analysis. In the score, plot letters depict nosespace sessions, and highly influential variables (VIP scores higher than 1.5) are represented by means of the corresponding rounded-up masses.

### 3.3. Headspace vs. Nospace

To perform an in-depth comparison between headspace and nosespace, a more thorough analysis of the two datasets was carried out. The headspace mass peaks used in this part of the analysis were a total of 105. These corresponded to mass peaks having a concentration higher than 1 ppbV and tentatively linked to a known coffee volatile compound (Table S3, Supplementary Material). These were sorted according to chemical class (e.g., pyrroles, carbonyls, sulfur compounds, etc.) and relative abundance. The same procedure was carried out on the 35 nosespace mass peaks. In this case, to calculate relative abundance, the area parameter was employed. The number of remaining NS mass peaks was in total 25, 28, and 27 for coffees A, B, and E, respectively. Coffee E contained  $m/z$  82.065 and 99.081 in addition to coffee A; coffee B also contained  $m/z$  98.064 in addition to coffees A and E.

The comparison between the HS and NS datasets is represented by means of three circular graphs, one for each coffee, as shown in Figure 3. In each graph, the inner circle represents the NS data; mass peaks are labeled by the respective exact mass values, ranked first by chemical class and then by relative abundance within each class, with values increasing in an anti-clockwise direction. Similarly, the outer circles depict the HS data;

each peak is represented by a dot, and whenever the HS mass peak is present in the NS as well, the dot is filled, and a line joins the two data points. Empty dots represent instead HS mass peaks that were not detected in NS. Chemical classes are represented by means of the different coloring of the two circles.

**Table 3.** Selected nosespace mass peaks and corresponding parameters (VIP > 1.5). Means and standard deviations are reported for each sample. *p*-values were obtained on the basis of one-way ANOVA and corrected, taking into account the false discovery rate. Superscript annotations are used to display differences between coffees; therefore, when two values are annotated by different letters, this denotes the pairwise statistically significant difference (Tukey's HSD).

Measured Mass <i>m/z</i> (Th)	Sum Formula	Tentative Identification	Parameter *	Coffee A	Coffee B	Coffee E	<i>p</i> -Value
68.056	C <sub>4</sub> H <sub>6</sub> N <sup>+</sup>	Pyrrole	Slope	0.008 ±	0.003 <sup>a</sup>	0.010 ±	0.031
			Area	119.32 ±	23.58 <sup>a</sup>	198.17 ±	0.149
79.049	C <sub>6</sub> H <sub>7</sub> <sup>+</sup>	Benzene/benzaldehyde fragment	Area	64.04 ±	30.26 <sup>a</sup>	122.81 ±	0.037
80.050	C <sub>5</sub> H <sub>6</sub> N <sup>+</sup>		Pyridine	Area	526.84 ±	175.12 <sup>a</sup>	1529.2 ±
82.070	C <sub>5</sub> H <sub>8</sub> N <sup>+</sup>	Methyl-pyrrole	Median	2.32 ±	0.96 <sup>a</sup>	6.39 ±	0.049
			Slope	0 ±	0 <sup>a</sup>	0.013 ±	<10 <sup>-3</sup>
			Area	0 ±	0 <sup>a</sup>	82.65 ±	<10 <sup>-3</sup>
			Median	0 ±	0 <sup>a</sup>	0.22 ±	<10 <sup>-3</sup>
			Final	0 ±	0 <sup>a</sup>	0.15 ±	<10 <sup>-3</sup>
			Maximum	0 ±	0 <sup>a</sup>	8.66 ±	0.004
			Area	0 ±	0 <sup>a</sup>	14.44 ±	<10 <sup>-3</sup>
98.074	C <sub>5</sub> H <sub>8</sub> ON <sup>+</sup>	Dimethyl-oxazole	Median	0 ±	0 <sup>a</sup>	0.06 ±	<10 <sup>-3</sup>
			Area	0 ±	0 <sup>a</sup>	0.01 ±	<10 <sup>-3</sup>
			Slope	0 ±	0 <sup>a</sup>	0.006 ±	<10 <sup>-3</sup>
			Final	0 ±	0 <sup>a</sup>	0.05 ±	<10 <sup>-3</sup>
			Maximum	0 ±	0 <sup>a</sup>	0.68 ±	<10 <sup>-3</sup>
			Area	0 ±	0 <sup>a</sup>	14.44 ±	<10 <sup>-3</sup>
			Final	0 ±	0 <sup>a</sup>	0.05 ±	<10 <sup>-3</sup>
99.082	C <sub>6</sub> H <sub>11</sub> O <sup>+</sup>	Hexenal/methyl-pentenone	Area	0 ±	0 <sup>a</sup>	54.32 ±	<10 <sup>-3</sup>
			Final	0 ±	0 <sup>a</sup>	0.23 ±	<10 <sup>-3</sup>
			Median	0 ±	0 <sup>a</sup>	0.30 ±	<10 <sup>-3</sup>
			Slope	0 ±	0 <sup>a</sup>	0.006 ±	<10 <sup>-3</sup>
			Maximum	0 ±	0 <sup>a</sup>	1.96 ±	0.002
125.065	C <sub>7</sub> H <sub>9</sub> O <sub>2</sub> <sup>+</sup>	guaiacol/methyl-benzenediol/furyl acetone	Area	37.73 ±	8.39 <sup>a</sup>	59.62 ±	0.198

\* Units of measure used for NS parameters: Area: ppbV·s; Maximum, Median, Final: ppbV; Slope: ppbV·s<sup>-1</sup>.

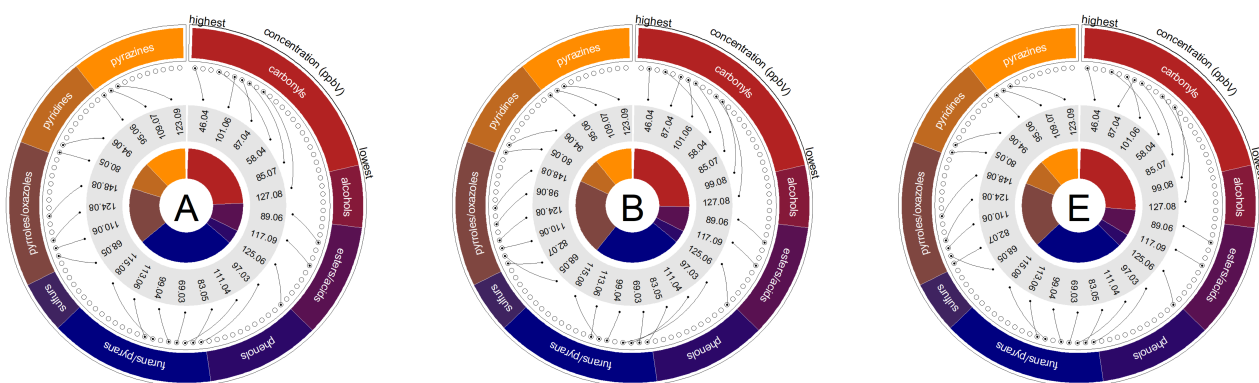


**Figure 3.** Circular plots. For each coffee, the composition of the headspace and the nosespace are represented by the outer and inner circles, respectively. Masses are sorted according to chemical class and relative abundance. When the same masses are detected in both experimental modes, these are linked by a continuous line.

Figure 3 shows that chemical groups that are abundant in HS remain prevalent in NS as well. For example, Figure 3 shows that carbonyls are the chemical class having the highest number of entries in both the HS and the NS. Carbonyls were also the most abundant in terms of overall concentration, with more than 50% of the total peak area in both cases (Table S3). The relative abundances of the chemical groups in the HS followed the same order for coffee A and E (carbonyls, furans/pyrans, esters/acids, alcohols,



pyrazines, pyridines, pyrroles, sulfur compounds, and phenols), but was different for coffee B (carbonyls, esters/acids, furans/pyrans, alcohols, pyridines, pyrroles, pyrazines, sulfur compounds, and phenols). The relative abundances of pyridines and pyrroles became dominant over pyrazines in coffee B, most probably due to the higher formation of  $m/z$  80.049 (pyridine) and 82.065 (methyl-pyrrole), with increasing roasting degree. Similarly, the relative abundances of these chemical groups in the NS followed the same order for coffees A and E (carbonyls, furans/pyrans, pyridines, pyrazines, pyrroles, esters/acids, and phenols) and a different order for coffee B (carbonyls, pyridines, furans/pyrans, pyrazines, pyrroles, esters/acids, and phenols).

Significant changes were observed between the HS and NS profiles of the coffee samples. Not surprisingly, a 2 to 40-fold signal reduction was observed when switching from HS to NS. For most chemical classes, this meant that the most intense HS peaks remained visible in NS, whereas the less abundant were not detectable anymore; this was the case for pyrazines, pyridines, pyrroles, furans, pyrans, and phenols. The situation was different for carbonyl compounds. While carbonyls as a chemical class remained very abundant in NS, the individual distribution did not necessarily reflect HS composition. Some mass peaks, most notably  $m/z$  87.044 (tentatively identified as butanedione/butyrolactone) and 127.076 and (3-ethyl-1-2-cyclopentanedione) were proportionally increased in the NS of all coffees, whereas  $m/z$  99.081 (hexenal/methyl-pentenone) was proportionally increased in coffee B and coffee E. On the other hand, mass peaks  $m/z$  73.061 (isobutanal/butanone), 87.080 (methyl-butanal), and 31.019 (formaldehyde), which were among the ten most abundant carbonyls in coffee HS, were not detectable in the nose-space of the three coffees. A similar situation could be highlighted when looking at the most abundant six esters in coffee HS and comparing this result with NS data;  $m/z$  89.060 (methyl-propanoate/hydroxy-butanone) and 117.091 (hexanoic acid) were proportionally increased, whereas  $m/z$  61.027 (acetic acid/methyl-formate), 75.042 (methyl-acetate/acetol), 103.074 (hydroxy-pentanone/methyl-butanoic acid), and 47.014 (formic acid) disappeared. Finally, alcohols and sulfur compounds were not at all represented within coffee NS, where they were not detectable.

Several reasons may lie behind the changes in the intensity of volatile compounds from headspace to nose-space, including dilution of the sample by saliva in the mouth (quite significant for small amounts of liquid samples), absorption of the volatile compounds by nasal epithelia and their interaction with oral mucosa and lung channels [24,25], the dilution of the volatiles with the exhaled breath [1,2,4], and biotransformation by saliva or nasal mucus enzymes [26].

In conclusion, this work presents a complete workflow for PTR-ToF-MS measurement of *in vitro* and *in vivo* aroma release, followed by data processing and analysis and including the comparison of the resulting HS and NS datasets. PTR-ToF-MS was able to provide a detailed profile of the three coffees in both analytical modes, differentiating the three products with  $\geq 92\%$  accuracy. The comparison between HS and NS data highlights that the latter presents a greatly simplified image of the coffee aroma profile. The question is whether retronasal perception is equally simpler than the orthonasal one and more focused on a few key aroma compounds, such as the ones related to the roasting degree. It must be noted that among compounds that are quantitatively well-represented within coffee nose-space, some, such as pyrazines, also have an important role in determining coffee aroma, whereas others, such as some furans, were found to have only a minor sensory impact [21]. Possible follow-up investigations might involve studies involving larger numbers of coffees or panelists or comparisons between instrumental, sensory data, and individual panelist physiological parameters.

**Supplementary Materials:** The following supporting information can be downloaded at: <https://www.mdpi.com/article/10.3390/app122010272/s1>, Table S1: Headspace mass peaks with concentration  $\geq 1$ ppbV; Table S2: Nose-space parameters; Table S3: Headspace and nose-space mass peaks: concentrations and tentative identifications.

**Author Contributions:** Conceptualization, L.N. and F.B.; methodology, A.R. and F.B.; software, A.R. and L.C.; validation, A.R., L.C. and F.B.; formal analysis, A.R. and L.C.; investigation, A.R. and L.C.; resources, L.N. and F.B.; data curation, A.R. and L.C.; writing—original draft preparation, A.R.; writing—review and editing, A.R., L.C., S.B., P.P., L.N. and F.B.; visualization, A.R.; supervision, S.B., P.P. and F.B.; project administration, S.B., P.P., L.N. and F.B.; funding acquisition, S.B., P.P., L.N. and F.B. All authors have read and agreed to the published version of the manuscript.

**Funding:** This research was funded by the Autonomous Province of Trento, grant number ADP 2022.

**Informed Consent Statement:** Informed consent was obtained from all subjects involved in the study.

**Data Availability Statement:** Not applicable.

**Conflicts of Interest:** The authors declare no conflict of interest.

## References

1. Linforth, R.; Martin, F.; Carey, M.; Davidson, J.; Taylor, A.J. Retronasal Transport of Aroma Compounds. *J. Agric. Food Chem.* **2002**, *50*, 1111–1117. [[CrossRef](#)] [[PubMed](#)]
2. Linforth, R.; Taylor, A. The Process of Flavour Release. In *Flavour in Food*; Elsevier: Amsterdam, The Netherlands, 2006; pp. 287–307, ISBN 978-1-85573-960-4.
3. Yeretian, C.; Pollien, P.; Lindinger, C.; Ali, S. Individualization of Flavor Preferences: Toward a Consumer-Centric and Individualized Aroma Science. *Compr. Rev. Food Sci. Food Saf.* **2004**, *3*, 152–159. [[CrossRef](#)] [[PubMed](#)]
4. Gierczynski, I.; Guichard, E.; Laboure, H. Aroma Perception in Dairy Products: The Roles of Texture, Aroma Release and Consumer Physiology. A Review. *Flavour Fragr. J.* **2011**, *26*, 141–152. [[CrossRef](#)]
5. Guichard, E. Interactions between Flavor Compounds and Food Ingredients and Their Influence on Flavor Perception. *Food Rev. Int.* **2002**, *18*, 49–70. [[CrossRef](#)]
6. Taylor, A.J.; Beauchamp, J.D.; Langford, V.S. Non-Destructive and High-Throughput—APCI-MS, PTR-MS and SIFT-MS as Methods of Choice for Exploring Flavor Release. In *Dynamic Flavor: Capturing Aroma Using Real-Time Mass Spectrometry*; ACS Symposium Series; American Chemical Society: Washington, DC, USA, 2021; Volume 1402, pp. 1–16.
7. Graus, M.; Yeretian, C.; Jordan, A.; Lindinger, W. In-Mouth Aroma: Breath-by-Breath Analysis of Nosespace by PTR-MS While Drinking Coffee. In Proceedings of the XIIIth Symposium on Atomic, Cluster and Surface Physics, Kitzbühel, Austria, 17–23 February 2002.
8. Barron, D.; Pineau, N.; Matthey-Doret, W.; Ali, S.; Sudre, J.; Germain, J.C.; Kolodziejczyk, E.; Pollien, P.; Labbe, D.; Jarisch, C.; et al. Impact of Crema on the Aroma Release and the In-Mouth Sensory Perception of Espresso Coffee. *Food Funct.* **2012**, *3*, 923–930. [[CrossRef](#)]
9. Romano, A.; Cappellin, L.; Ting, V.; Aprea, E.; Navarini, L.; Gasperi, F.; Biasioli, F. Nosespace Analysis by PTR-ToF-MS for the Characterization of Food and Tasters: The Case Study of Coffee. *Int. J. Mass Spectrom.* **2014**, *365–366*, 20–27. [[CrossRef](#)]
10. Charles, M.; Romano, A.; Yener, S.; Barnabà, M.; Navarini, L.; Märk, T.D.; Biasoli, F.; Gasperi, F. Understanding Flavour Perception of Espresso Coffee by the Combination of a Dynamic Sensory Method and In-Vivo Nosespace Analysis. *Food Res. Int.* **2015**, *69*, 9–20. [[CrossRef](#)]
11. Colzi, I.; Taiti, C.; Marone, E.; Magnelli, S.; Gonnelli, C.; Mancuso, S. Covering the Different Steps of the Coffee Processing: Can Headspace VOC Emissions Be Exploited to Successfully Distinguish between Arabica and Robusta? *Food Chem.* **2017**, *237*, 257–263. [[CrossRef](#)]
12. Yener, S.; Romano, A.; Cappellin, L.; Märk, T.D.; Del Pulgar, J.S.; Gasperi, F.; Navarini, L.; Biasioli, F. PTR-ToF-MS Characterisation of Roasted Coffees (C. Arabica) from Different Geographic Origins. *J. Mass Spectrom.* **2014**, *49*, 929–935. [[CrossRef](#)]
13. Yener, S.; Romano, A.; Cappellin, L.; Granitto, P.M.; Aprea, E.; Navarini, L.; Märk, T.D.; Gasperi, F.; Biasioli, F. Tracing Coffee Origin by Direct Injection Headspace Analysis with PTR/SRI-MS. *Food Res. Int.* **2015**, *69*, 235–243. [[CrossRef](#)]
14. Lopes, G.R.; Petronilho, S.; Ferreira, A.S.; Pinto, M.; Passos, C.P.; Coelho, E.; Rodrigues, C.; Figueira, C.; Rocha, S.M.; Coimbra, M.A. Insights on Single-Dose Espresso Coffee Capsules' Volatile Profile: From Ground Powder Volatiles to Prediction of Espresso Brew Aroma Properties. *Foods* **2021**, *10*, 2508. [[CrossRef](#)]
15. Cappellin, L.; Biasioli, F.; Granitto, P.M.; Schuhfried, E.; Soukoulis, C.; Costa, F.; Märk, T.D.; Gasperi, F. On Data Analysis in PTR-TOF-MS: From Raw Spectra to Data Mining. *Sens. Actuators B Chem.* **2011**, *155*, 183–190. [[CrossRef](#)]
16. Cappellin, L.; Biasioli, F.; Fabris, A.; Schuhfried, E.; Soukoulis, C.; Märk, T.D.; Gasperi, F. Improved Mass Accuracy in PTR-TOF-MS: Another Step towards Better Compound Identification in PTR-MS. *Int. J. Mass Spectrom.* **2010**, *290*, 60–63. [[CrossRef](#)]
17. Cappellin, L.; Biasioli, F.; Schuhfried, E.; Soukoulis, C.; Märk, T.D.; Gasperi, F. Extending the Dynamic Range of Proton Transfer Reaction Time-of-Flight Mass Spectrometers by a Novel Dead Time Correction: Extending the Dynamic Range of PTR-TOF-MS. *Rapid Commun. Mass Spectrom.* **2011**, *25*, 179–183. [[CrossRef](#)]
18. Lindinger, W.; Hansel, A.; Jordan, A. On-Line Monitoring of Volatile Organic Compounds at Pptv Levels by Means of Proton-Transfer-Reaction Mass Spectrometry (PTR-MS) Medical Applications, Food Control and Environmental Research. *Int. J. Mass Spectrom. Ion Process.* **1998**, *173*, 191–241. [[CrossRef](#)]

19. Chong, I.-G.; Jun, C.-H. Performance of Some Variable Selection Methods When Multicollinearity Is Present. *Chemom. Intell. Lab. Syst.* **2005**, *78*, 103–112. [[CrossRef](#)]
20. R Core Team. *R: A Language and Environment for Statistical Computing*; R Foundation for Statistical Computing: Vienna, Austria, 2020.
21. Schenker, S.; Heinemann, C.; Huber, M.; Pompizzi, R.; Perren, R.; Escher, R. Impact of Roasting Conditions on the Formation of Aroma Compounds in Coffee Beans. *J. Food Sci.* **2002**, *67*, 60–66. [[CrossRef](#)]
22. Del Terra, L.; Lonzarich, V.; Asquini, E.; Navarini, L.; Graziosi, G.; Suggi Liverani, F.; Pallavicini, A. Functional Characterization of Three *Coffea Arabica* L. Monoterpene Synthases: Insights into the Enzymatic Machinery of Coffee Aroma. *Phytochemistry* **2013**, *89*, 6–14. [[CrossRef](#)]
23. Flament, I.; Bessi re-Thomas, Y. *Coffee Flavor Chemistry*; Wiley: Chichester, UK; New York, NY, USA, 2002; ISBN 978-0-471-72038-6.
24. Buettner, A.; Beer, A.; Hannig, C.; Settles, M.; Schieberle, P. Physiological and Analytical Studies on Flavor Perception Dynamics as Induced by the Eating and Swallowing Process. *Food Qual. Prefer.* **2002**, *13*, 497–504. [[CrossRef](#)]
25. Mu oz-Gonz lez, C.; Brule, M.; Martin, C.; Feron, G.; Canon, F. Molecular Mechanisms of Aroma Persistence: From Noncovalent Interactions between Aroma Compounds and the Oral Mucosa to Metabolization of Aroma Compounds by Saliva and Oral Cells. *Food Chem.* **2022**, *373*, 131467. [[CrossRef](#)]
26. Ijichi, C.; Wakabayashi, H.; Sugiyama, S.; Ihara, Y.; Nogi, Y.; Nagashima, A.; Ihara, S.; Niimura, Y.; Shimizu, Y.; Kondo, K.; et al. Metabolism of Odorant Molecules in Human Nasal/Oral Cavity Affects the Odorant Perception. *Chem. Senses* **2019**, *44*, 465–481. [[CrossRef](#)]